The Iraqi Journal For Mechanical And Material Engineering, Vol.12, No.4, 2012

NUMERICAL STUDY OF MIXED CONVECTION OF AIR IN THE ENTRANCE REGION OF VERTICAL CONCENTRIC ANNULUS

Asmaa Ali Hussein
Lecturer
Foundation Of Technical Education

ABSTRACT

Numerical results of a finite difference scheme are presented for the developing mixed forced – free laminar boundary layer flow in a vertical concentric annulus with a uniformly heated inner cylinder. The effect of a superimposed aiding or opposing free convection on the developing velocity profiles is investigated for a fluid with Pr=0.7 over the ranges of heat flux $50 \leq q \leq 250$ (W/m^2), Reynolds number $200 \leq Re \leq 1200$, and radius ratio $0.2 \leq N \leq 0.9$. The effects of heat flux , Reynolds number , and radius ratio on the developing of the axial velocity profiles , temperature profiles , and local Nusselt number along annulus are discussed. Results show that the growth of the thermal boundary layer along the annulus increases as heat flux increases and Reynolds number decreases. Computer program in Fortran language was developed to carry out the necessary calculation.

الخلاصة:

عرضت نتائج عددية أجريت بطريقة الفروقات المحددة لجريان الطبقة المتاخمة الطباقي الحر- القسري المختلط بمنطقة التشكيل لتجويف حلقي متمركز عمودي بأسطوانة داخلية مسخّنة تسخين منتظم. تم التحري عن التأثير الإضافي للحمل الحر المساعد أو المعاكس على أشكال السرعة المشكّلة لمائع ذو Pr=0.7 لمديات من $50 \leq q \leq 250$ (W/m^2) , $200 \leq Re \leq 1200$, و نسبة نصف القطر $0.2 \leq N \leq 0.9$. تم مناقشة تأثيرات الفيض الحراري، رقم رينولدز، و نسبة نصف القطر على تشكيل أشكال السرعة المحورية، أشكال درجات الحرارة، و رقم نسلت الموقعي خلال التجويف الحلقي. بينت النتائج أن نمو الطبقة المتاخمة الحرارية خلال التجويف الحلقي يزداد بزيادة الفيض الحراري و نقصان رقم رينولدز. طور برنامج حاسوبي بلغة (Fortran) لتنفيد الحسابات اللازمة.

Key Words: Heat Transfer, Combined (Mixed) Convection, Annulus, Cylinder.

INTRODUCTION

Heat transfer takes place between a solid surface and a fluid whenever a temperature difference exists. When mixing of the fluid particles occurs, the heat is transferred by convection. The latter may either be forced or natural depending on whether the fluid motion is imposed or whether it occurs because of a difference in density**.** Mixed free and forced convection which is characterized by Richardson number (Ri) which represents the ratio of buoyancy force (Gr) and inertial force (Re^2). There are many employments for heat transfer by mixed convection in concentric annular tubes because of special importance in many industrial engineering applications for examples; double pipe heat exchangers designed for chemical process, food industrial, heating of process fluids, the cooling of electrical cables and nuclear fuel rods, and the collection of solar energy ***Holland and Moores 1970***. ***El-Sharrawi and Sarhan 1980***, studied mixed convection of upward and downward air flow in a vertical annulus of radius ratio (0.5, 0.8, and 0.9) and $\Pr = 0.7$ with a flat velocity profile at the entrance and under two cases .For first case, the outer cylinder was isothermal while the inner cylinder was adiabatic under ($-700 \le Gr/Re_d \le 1600$); while for the second case, the inner cylinder was isothermal and the outer cylinder was adiabatic under ($-200 \le Gr/Re_d \le 800$). They noticed that when the free convection opposed the forced flow (heating with down flow or cooling with up flow) there exists a possibility of reversal flow near the heated boundary while such a reversal flow may occurred near the insulated wall if the free convection was aiding the forced flow. Steady-state, fully developed velocity and temperature fields in mixed convection through a horizontal annulus (radius ratio equal 0.8), with a prescribed constant heat flux on the inner cylinder and an adiabatic outside cylinder, were analyzed by ***Kaviany 1986***, using finite difference approximation over the range of $10^5<Ra<10^9$ and (Pr = 0.7,7 and 70). Results of the inner surface temperature, development of axial velocity profiles, and the effect of the buoyancy on the radial temperature distribution along the annulus were calculated. Numerical solutions for the problem of steady laminar combined convection flows in vertical annular ducts were presented by ***Heggs et. al 1988***. The axial diffusion terms were assumed to be negligible in the governing equations and the resulting parabolic equations were solved by using an implicit finite difference scheme and a marching solution technique. Constant wall temperature boundary conditions were used and investigations were restricted to the case $(\Pr = 0.72)$. Large ranges of values of the governing parameters (Gr/Re) and radius ratio were considered $(-90 \le Gr/Re_d \le 125)$ and $(0.1 \le N \le 0.99)$. For large values of the ratio (Gr/Re) reverse flow was presented in the fluid. ***Falah 1993*** performed numerical investigation of axially symmetric laminar upward air flow in an entrance region of a vertical annulus by solving in two direction the continuity, momentum and energy equations using implicit finite difference method and Gauss elimination technique. The investigation has covered Re range from 300 to 1200, heat flux varied from 90 W/m^2 to 680 W/m^2. Results showed that the local Nusselt number increases as heat flux increases. ***Nieckele and Patankar 2001*** presented a numerical study for the fully developed region of the buoyancy affected flow with an axial laminar flow in a horizontal annular pipe of radius ratio $(N = 0.2, 0.33, 0.5 \text{ and } 0.66)$, $(10^4 \le Ra \le 10^7)$, and $(Ra/(Re_d \times Pr)^2 < 1)$.

The inner wall was heated isothermally while the outer wall was considered adiabatic. Results showed that at a given Ra, the effect of buoyancy on the heat transfer coefficient was stronger at higher Pr. The local heat transfer coefficients on the inner cylinder became highly non uniform at high Ra, while the lowest value being at the top of the cylinder. Steady, laminar, mixed convection in a fully developed region of horizontal concentric annuli was investigated numerically for case of non-uniform circumferential heating by ***Habib and Negm 2001*** **.**Two heating conditions were studied, one in which a 180 arc encompassing the top half of inner surface of the inner cylinder heated uniformly while the bottom half considered insulated, and the other in which the heated and the insulated surfaces were reversed. The fluid flow and the heat transfer characteristics were found to be affected by the heating conditions. ***Coney and EL-Shaarawi 2005*** used the finite difference analysis for laminar air flow in an annulus of radius ratio (0.1, 0.5, and 0.9) and Pr =0.7 with a simultaneously developing flow hydrodynamically and thermally. Two cases of boundary conditions were studied, for (case one) the outer cylinder was isothermal and the inner cylinder was adiabatic with uniform fluid temperature entrance and the opposite state at (case two) was considered as a boundary conditions. A comparison between the local Nasselt numbers and the mixing cup temperature along the annulus were investigated. Results showed how much error can be introduced for the case of gases (Pr=0.7) if the heat transfer was calculated by assuming a fully developed profile from the entrance. ***Hashimoto et. al 2005,*** studied this phenomena for both upward and downward helium gas flow with $\mathrm{Pr} = 0.671$, with a simultaneously developing hydrodynamic and thermal boundary layer in a vertical annulus of (0.9) radius ratio under isothermal or constant heat flux inner wall and adiabatic outer wall, for isothermal wall case $(0 \le \mathrm{Gr}/\mathrm{Re}_d \le 1500)$, and constant heat flux case $(0 \le \mathrm{Gr}/\mathrm{Re}_d \le 4000)$. They concluded that the critical condition of $\mathrm{Gr}/\mathrm{Re}_d$ effect on the reversal flow and the effect of property variations on both Nusselt number and friction factor for downward flow was much smaller than that for upward flow. ***Shaik 2005*** analyzed the hydrodynamic behavior of mixed convection flow under isothermal boundary conditions along a circular channel. The pressure and pressure gradient variation along the channel (from the entrance till the fully developed region) was obtained numerically. Moreover, critical values of the buoyancy parameter $\mathrm{Gr}/\mathrm{Re}_d$ were determined and equal (0, 116.21, 200, 300, 400) while the radius ratio (0.1, 0.3, 0.5 and 0.7). The hydrodynamic and heat transfer parameters of relevant importance were also presented. A numerical study of steady state, simultaneously developing laminar mixed convection in a vertical double pipe heat exchanger was conducted by ***Voicu et al 2007*** for upward parallel flow. The results showed that the flow reversal occurs in the warm fluid for Richardson number greater than equal to one. The coupled phenomenon of opposing mixed convection and radiation within differentially heated eccentric horizontal cylindrical annulus was numerically simulated by ***Sakar and Mahabatra 2009***. The radiation transfer contributed from the participating medium was obtained by solving the nonlinear integro-differential radiative transfer equation using discrete ordinate method. It was found that substantial changes occur in isotherms as well as in flow patterns, when the Richardson number was allowed to vary in the range of 0.01–1.

Of particular interest to the present investigation is the variation of fluid density with temperature. A change in fluid density causes a change in the gravitational body force on a volume of the fluid. At low Reynolds number gravitational body forces play an important role in determining flow regime. Under certain circumstances body forces created under the action of temperature-dependent fluid density may change a forced laminar flow to the so-called combined forced-free, or mixed convection laminar flow. The present study is an attempt to investigate the free convection effects on the developing forced laminar upward or downward flow in a vertical annulus with uniformly heated inner cylinder and adiabatically insulated stationary outer cylinder.

GOVERNING EQUATIONS

The configuration of this problem is shown in **Fig. 1** which represents two concentric cylinder with uniformly heated inner cylinder and adiabatic outer cylinder**.** Assuming steady, axisymmetric , laminar flow of an incompressible Newtonian fluid, no internal heat generation, constant physical properties except the density which only varies in the gravitational body force term according to the Boussinesq approximation , neglecting viscous dissipation and axial conduction of heat , assuming Re>>0 , and applying the Prandtl boundary layer assumptions. The governing equations of mixed convection in the entrance region of a vertical annulus are as follows ***EI-Shaarawi*** and ***Sarhan1980***:

$$\frac{\partial (rv)}{\partial r} + \frac{\partial (ru)}{\partial z} = 0 \tag{1}$$

$$\rho_i \left(v\frac{\partial u}{\partial r} + u\frac{\partial u}{\partial z} \right) = -\frac{\partial p}{\partial z} \mp \rho_i g \left[1 - \beta (t - t_i) \right] + \frac{\mu}{r}\frac{\partial}{\partial r}\left(r\frac{\partial u}{\partial r} \right) \tag{2}$$

$$\rho_i c \left(v\frac{\partial t}{\partial r} + u\frac{\partial t}{\partial z} \right) = \frac{k}{r}\frac{\partial}{\partial r}\left(r\frac{\partial t}{\partial r} \right) \tag{3}$$

The minus and plus signs in the gravitational term of eq. (2) apply respectively to upward and downward flows, taking into consideration that the force acts in the negative z-direction in case of an upward flow and vice versa in case of a downward flow.

Dissociating the pressure into the usual two components, i.e.

$$p = \bar{p} + p_s = \bar{p} \mp \rho_i g z \tag{4}$$

in which the minus and plus signs apply respectively to upward and downward flows. Eq. (2) can be written as follows:

$$\rho_i\left(v\frac{\partial u}{\partial r}+u\frac{\partial u}{\partial z}\right)=-\frac{\partial \overline{p}}{\partial z}\pm\rho_i g\beta\left(t-t_i\right)+\frac{\mu}{r}\frac{\partial}{\partial r}\left(r\frac{\partial u}{\partial r}\right) \tag{5}$$

Using the dimensionless parameters given in the nomenclature. Eqs. (1), (3), and (5) can be replaced by the following dimensionless forms:

$$\frac{\partial V}{\partial R}+\frac{V}{R}+\frac{\partial U}{\partial Z}=0 \tag{6}$$

$$V\frac{\partial U}{\partial R}+U\frac{\partial U}{\partial Z}=-\frac{\partial P}{\partial Z}\pm 2\frac{Gr}{Re}T+\frac{\partial^2 U}{\partial R^2}+\frac{1}{R}\frac{\partial U}{\partial R} \tag{7}$$

$$V\frac{\partial T}{\partial R}+U\frac{\partial T}{\partial Z}=\frac{1}{Pr}\left(\frac{\partial^2 T}{\partial R^2}+\frac{1}{R}\frac{\partial T}{\partial R}\right) \tag{8}$$

The three coupled eqs. (6-8) are subjected to the following boundary conditions:

1. For $Z\geq 0$ and $R=N$,
   $U=V=0$ and $\partial T/\partial R=(1-N)(r_2/L)^4$ (9-a)

2. For $Z\geq 0$ and $R=1$,
   $U=V=0$, $\partial T/\partial R=0$ (9-b)

3 .For $Z=0$,
   $U=1$,$V=0$, $P=0$, $T=0$ (9-c)

The integral continuity equation can be written in the form:

$$\int_N^1 RU \quad dR=\frac{1}{2}\left(1-N^2\right) \tag{10}$$

FURTHER CALCULATIONS

Knowing that the temperature profiles from the numerical solution of energy, the mixing cup temperature and the local Nusselt number at any cross-section can be calculated. The mixing cup temperature at any cross section is defined by:

$$t_b=\frac{\int_{r_1}^{r_2} t \quad u \quad r \quad dr}{\int_{r_1}^{r_2} u \quad r \quad dr} \tag{11}$$

or, in dimensionless form

$$T_b = \frac{\int_N^1 T \quad U \quad R \quad dR}{\int_N^1 U \quad R \quad dR} \tag{12}$$

The local Nusselt numbers at any cross-section in the annular gap are defined respectively as follows:

$$Nu_z = \frac{q \quad D_h}{k(t_{s_z} - t_{b_z})} \tag{13}$$

$$Nu_z = \frac{D_h \quad \left(\frac{\partial t}{\partial r}\right)_{r = r_1}}{(t_{s_z} - t_{b_z})} \tag{14}$$

or , in dimensionless form, Eq.(14) can be written as follows:

$$\mathrm{Nu}_z = \frac{2(1-\mathrm{N})\left(\frac{\partial \mathrm{T}}{\partial \mathrm{R}}\right)_{\mathrm{R} = \mathrm{N}}}{(\mathrm{T}_{s_z} - \mathrm{T}_{b_z})} \tag{15}$$

The average Nusselt number is defined as:

$$Nu_m = \frac{1}{L}\int_o^L Nu_z dz \tag{16}$$

NUMERICAL METHOD OF SOLUTION

Considering the mesh net work of **Fig. 2**. Basically, the flow region is divided into grid network (ΔR, ΔZ) so that the different terms in the governing equations expressed in finite difference form are subjected to the imposed boundary conditions**.** It may be worth mentioning that, the chosen finite difference approximations are not perfectly symmetrical nor are they of the same form in all the equations. This is done so as to insure stability of the numerical solution and to enable the equations to be solved in the manner that will be discussed later . In the following finite difference equations (Eqs. (6-8) and Eq. (10)) the variables with subscript j+1 represent the unknowns and those with subscript j are known (**El-Shaarawi and Serhah 1980 and Coney and El-Shaarawi 2005**) as follows:

$$\frac{V_{i+1,j+1} - V_{i,j+1}}{\Delta R} + \frac{V_{i+1,j+1} + V_{i,j+1}}{2[N + (i-1)\Delta R]} + \frac{(U_{i+1,j+1} + U_{i,j+1}) - (U_{i+1,j} + U_{i,j})}{2\Delta Z} = 0 \tag{17}$$

$$V_{i,j}\frac{U_{i+1,j+1} - U_{i-1,j+1}}{2\Delta R} + U_{i,j}\frac{U_{i,j+1} - U_{i,j}}{\Delta Z} = \frac{P_{i,j} - P_{i,j+1}}{\Delta Z} + \frac{2Gr}{Re}T_{i,j+1} +$$

$$\frac{U_{i+1,j+1}-2U_{i,j+1}+U_{i-1,j+1}}{\Delta R^{2}}+\frac{1}{N+(i-1)\Delta R}\frac{U_{i+1,j+1}-U_{i-1,j+1}}{2\Delta R} \tag{18}$$

$$V_{i,j}\frac{T_{i+1,j+1}-T_{i-1,j+1}}{2\Delta R}+U_{i,j}\frac{T_{i,j+1}-T_{i,j}}{\Delta Z}=\frac{1}{Pr}\frac{\left(T_{i+1,j+1}-2T_{i,j+1}+T_{i-1,j+1}\right)}{(\Delta R)^{2}}+\frac{1}{N+(i-1)\Delta R}\times \frac{T_{i+1,j+1}-T_{i-1,j+1}}{2\Delta R} \tag{19}$$

$$\Delta R\sum_{i=2}^{n}U_{i,j}\left[N+(i-1)\Delta R\right]=\frac{1}{2}\left(1-N^{2}\right) \tag{20}$$

The numerical solution of these equations is obtained by first selecting values of Pr=0.7, heat flux $50 \le q \le 250$ (W/m^2) , Reynolds number $200 \le Re \le 1200$, and radius ratio $0.2 \le N \le 0.9$. Then , starting with j=1 (entrance cross-'section) and applying eq.(19) for i=2,3,…..,n yields (n-1) simultaneous linear algebraic equations which when solved by Gauss-Siedel elimination method give the unknown values of T’s at all points of the second cross-section. Now, applying eq. (18) with j=2,3,…..,n+1 and eq. (20) with i=2,3,….,n to the entire cross-section, we get 2n equations which when solved, by means of a special form of the Gauss-Siedel elimination scheme, give the unknown values of U’s and P’s at all points of the second cross-section. Using the computed values of U’s and applying eq. (17) we get the unknown values of V’s at the grid points of the second cross-section. The known values of T, U, V and P were then used as input data to solve the next axial step.

The introduction of second derivative of velocity and temperature in the axial direction means that three axial positions were involved in the finite difference approximation, two positions (suffices "n-1" and "n") were known and one (suffices "n+1") was unknown. After solution of a given step, the old values at "n" and "n+1" become the new values at "n-1" and "n" respectively and old "n-1" data redundant. Computer program in Fortran language was developed to carry out the necessary calculation as shown in **Fig.3**.

RESULTS AND DISCUSSION

Velocity Profile

Development axial velocity profiles along the vertical annulus axis with the uniformly heated inner cylinder are shown in **Figs.4-9. Fig.4**. shows development of axial velocity profile along the annulus axis for aiding flow case, N=0.5, q=100 W/m^2 , Re=200. It is obvious that when the free convection aids the forced flow the fluid accelerates near the heated wall and decelerates near the opposite insulated wall. This behavior can be explained as follows: the high effect of natural convection causes a steep temperature gradient near the heated surface. As a result, an appreciable density change (the fluid will be lighter in this region) creates a rapid growth of thermal boundary layer with the annulus length which causes an increasing of the axial velocity in this region. On the other hand, there is no significant variation of the temperature in the region bounded between annular gap core towards the outer wall. As a result, a decreasing of the axial velocity will be obtained in this region. Figure shows also that, as the flow progresses downstream, the axial velocity begins to increase further towards the outer wall even reaches negative value leads to obtaining a limited amount of reversed flow near the outer wall.

If the Reynolds number increases to 1000 at the same input conditions as shown in **Fig.5.**, the effect of free convection will decreases and the maximum axial velocity diverges slightly from the heated wall towards the annular gap core and the decelerating will decreases near the outer wall because of the dominant forced convection in the heat transfer process.

Fig.6 shows the effect of inner wall heat flux on the axial velocity profile for N=0.5, Re=500 and at Z=0.04628. The increasing of heat flux creates an acceleration in the axial flow near the heated surface and deceleration near the opposite adiabatic wall, even reaches a negative values causes a limited amount of reversed flow in a quite small region. This figure shows also that at R=0.75 (i.e., RR=0.4375) the axial velocities for a various selected values of heat flux are equal.

The developing axial velocity profile for opposing flow case, N=0.5, q=50 & 150 W/m^2 , Re=700 & 1200; are shown in **Fig.7** & **Fig.8** respectively. It is evident from these two figures that, at the entrance the shape of the axial velocity profile is a parabola then the maximum velocity bias towards the outer wall as the flow progresses further downstream. This prediction (as explained before) can physically be attributed to the fact that, when the free convection opposes the forced flow, the fluid accelerates near the outer adiabatic wall, and due to the continuity principle, decelerates near the heated boundary. As a result a reverse flow occurs in this region and vice versa when the free convection aids the forced flow. This fact appears evidently in **Fig.9** which represents a comparison between aiding & opposing flow case , N=0.5, q=100 W/m^2 and Re=500.

Temperature Profile

The developing of temperature profiles along the vertical annulus are shown in **Fig.10** which represents for aiding flow case, N=0.5, q=100 W/m^2 and Re=200. The figure depicted a steep temperature gradient near the heated wall and the thickness of the thermal boundary layer gradually increases as the flow moves from annulus inlet toward annulus exit. It can be seen that there is relatively high temperature variation causes an appreciable density change, which creates a rapid growth of the thermal boundary layer with annulus exit.

The thickness of thermal boundary layer decreases due to decreasing of temperature values if the Reynolds number increases to 1000 as shown in **Fig. 11** because of dominant forced convection in the heat transfer process.

Fig. 12 shows the effect of heat flux on the temperature profiles developing along the vertical annulus for aiding flow case, Re=500 and at Z=0.04628. It can be seen that the growth of the thermal boundary layer along the annulus increases as the heat flux increases. This means that the effect of natural convection seems to be higher as the heat flux increases.

Temperature profiles development along the annulus axis, for opposing flow case, N=0.5, Re=1200, q=50 W/m^2 and 150 W/m^2 are shown in **Fig. 13** and **Fig. 14**; respectively. The behavior of the temperature profiles development in these two figures is the same as in aiding flow case.

Local Nusselt Number

The effect of radius ratio on the Nu_z variation along Z-axis is shown in **Fig. 15** which represents for aiding flow case, Re=500 and q=100 W/m^2; and in **Fig. 16** which represents for opposing flow case, Re=850 and q=75 W/m^2. It can be seen that the heat is removed most efficiently from the inner heated wall for small values of N because for small N the gap in the annulus would be relatively very large and even if heat flows into the fluid at a high rate it would be carried off downstream before it was able to penetrate very far across the gap.

Fig. 17 represents for aiding flow case, N=0.5 & Re=500; and shows the significant effects of a superimposed free convection on the heat transfer characteristics of a developing laminar annular flow. It is clear that, at the entrance there is no effect of the increasing of heat flux on the Nu_z at the same value of Z, until a certain point after which the effects of free convection appear and the values of Nu_z increases as heat flux increases at the same value of Z.

Validation of Present work

Figs.(18, 19 & 20) represent the development of axial velocity profile, temperature profile and local Nusselt number; respectively, along annulus obtained by ***Falah 1993***. As shown in these figures the trend and behavior of fluid and heat transfer are relatively agree with the present results especially in **Figs.(5, 11 and 17).**

Conclusions

1. The fluid accelerates near the heated wall and decelerates near the opposite insulated wall in aiding flow case and vice versa in opposing flow case.
2. The growth of the thermal boundary layer along the annulus increases as heat flux increases and Reynolds number decreases.
3. The thickness of thermal boundary layer decreases due to decreasing of temperature values as Reynolds number increases more than 1000.
4. There is no effect of the increasing of heat flux at the annulus entrance then the heat transfer process improves downstream as the heat flux increases because of the strong natural convection.
5. The heat transfer process improves as radius ratio decreases.

REFERENCES

Holland F.A. , M.moores R.M., Wastor F.A and wilkingson J. K] "heat transfer" Heinemann Educational Books, Loondon,(1970).

El-Shaarawi M. A. and Sarhan A., "Free convection effects on the developing laminar flow in vertical concentric annuli "J. Heat Transfer, Vol. 102, pp.617-622, November, 1980.

Kaviany M.," Laminar combined convection in a horizontal annulus subjected to constant heat flux inner wall and adiabatic outer wall", J. Heat Transfer, Vol.108, pp. 392-397, May, 1986.

Heggs and Ingham "Laminar flow combined in vertical annuli", Proceeding of the 8th Int. Heat Transfer Conference, Munchen, Fed. Rep.of Germany, Vol.2, pp. 941-956, 1988.

Falah , "Combined free and forced convection in an inclination annulus " , M. Sc. Thesis, University of Basra, College of Engineering, Mechanical Department, 1993.

Nieckele A. O. and Patankar S. V.," Laminar mixed convection in a concentric annulus with horizontal axis," J. Heat Transfer, 2001.

Habib M. A. and Negm A. A. A. , " Laminar mixed convection in horizontal concentric annuli with non-uniform circumferential heating " , J. Heat and mass Transfer, Vol. 37, pp. 427-435, Numbers 4-5,July, 2001.

Coney J. E. R. and El-Shaarawi M. A. I. ,"Finite difference analysis for laminar flow heat transfer in concentric annuli with simultaneously developing hydrodynamic and thermal boundary layers " , Int. Journal for Numerical Method in Engineering, 20 Jun / 2005.

Hashimoto K., Akino N., and Kawamura H., "Combined forced- free convection heat transfer to a highly heated gas in a vertical annulus" ,Int. J. Heat Mass Transfer, 2005.

Shaik Samivullah, "Laminar mixed convection in vertical channels" M. Sc. Thesis, King Fahd University of Petroleum and Minerals, Mechanical Engineering, 2005.

Voicu, I, More, T., Galanis, N., Miriel, J., and Colda, I., "Mixed convection in a vertical double pipe heat exchanger", Int. J. Thermal Science, Vol. 46, Issue 6, pp.540-550, June 2007.

Sarkar, A. and Mahapatra, S. K. ,"Opposing mixed convection and its interaction with radiation inside eccentric horizontal cylindrical annulus", Int. Journal for Numerical Methods in Fluids, Volume 61, Issue 3, pp. 291–310, 30 September 2009.

NOMENCLATURE

b, annular gap width , (r_2-r_1) , m ;
c, specific heat of fluid at constant pressure , J/kg. ^oC;
D_h, hydraulic diameter of annulus , $2b = 2(r_2-r_1)$, m;
g , gravitational body force per unit mass , m/s^2;
Gr , modified Grashof number , $qg\beta L^4/k\nu^2$;

h , local heat transfer coefficient based on area of heated surface , $q/(t_{s_z} - t_b)$, $W/m^2.^oC$;
L , annulus height, m ;
k , thermal conductivity of fluid, $W/m.^oC$;
n , number of radial increments in the numerical mesh network ;
N , annulus radius ratio ,r_1/r_2 ;
Nu , local Nusselt number ;
p , pressure of fluid at any point, N/m^2 ;
p_i , pressure of fluid at annulus entrance, N/m^2;
p_s , hydrostatic pressure , $\pm \rho_i g z$, N/m^2 ;
$\overline{p}$, pressure defect at any point , $p-p_s$, N/m^2 ;
P, dimensionless pressure defect at any point , $(\overline{p}-p_i)/\rho_i u_i^2$;
Pr, Prandtl number , $\mu c/k$;
q, heat flux, W/m^2;
r, radial coordinate ;
r_1, inner radius, m ;
r_2, outer radius, m ;
R, dimensionless radial coordinate , r/r_2 ;
Re , Reynolds number , $u_i D_h/\nu$;
RR, dimensionless radial coordinate , $r-r_1/r_2-r_1$;
t , fluid temperature, ^oC ;
t_b , mixing cup temperature over any cross-section , $\int_{r_1}^{r_2} u\,t\,r\,dr \Big/ \int_{r_1}^{r_2} u\,r\,dr$, ^oC;
t_s , surface temperature, ^oC;
t_i , fluid temperature at annulus entrance, ^oC ;
T, dimensionless temperature , $(t-t_i)kbr_2^2/qL^4$;
T_b , dimensionless mixing cup temperature , $(t_b-t_i)kbr_2^2/qL^4$;
u , axial velocity, m/s ;
u_i , entrance axial velocity , $\int_{r_1}^{r_2} u r\,dr \Big/ \int_{r_1}^{r_2} r\,dr$, m/s;
U, dimensionless axial velocity , u/u_i ;
v , radial velocity, m/s;
V, dimensionless radial velocity , $v\,r_2/\nu$;
z , axial coordinate ;
Z, dimensionless axial coordinate , $2z(1-N)/r_2\,Re$

Greek symbols

β , volumetric coefficient of thermal expansion, 1/k ;
ρ , fluid density , $\rho_i[1-\beta(t-t_i)]$, kg/m^3 ;
ρ_i , fluid density at the entrance temperature, kg/m^3 ;
μ , dynamic viscosity of fluid, $N.s/m^2$;
ν , kinematic viscosity of fluid, m^2/s.

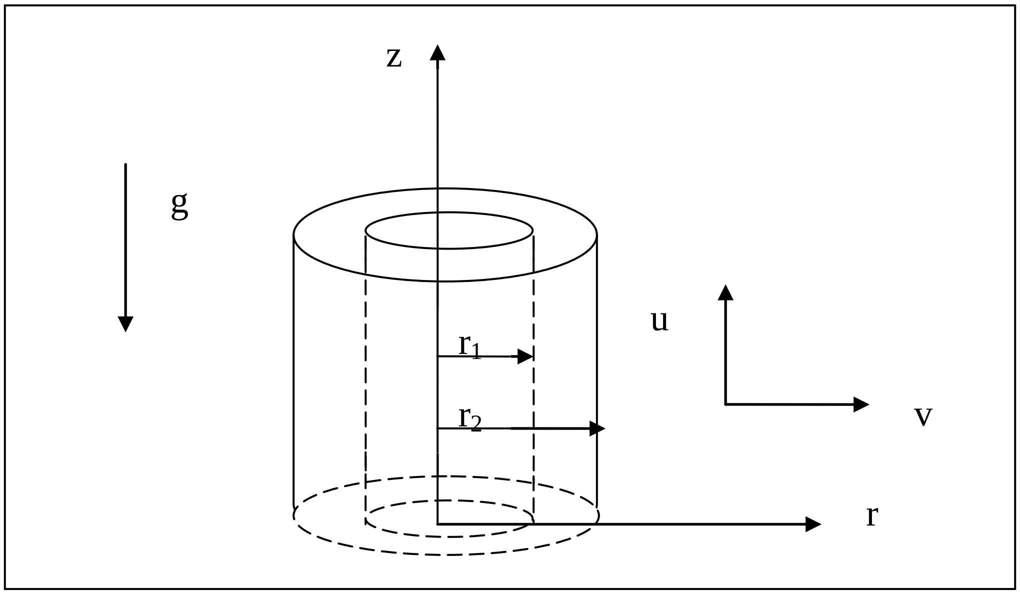

Fig.1: Two-dimensional annular geometry.

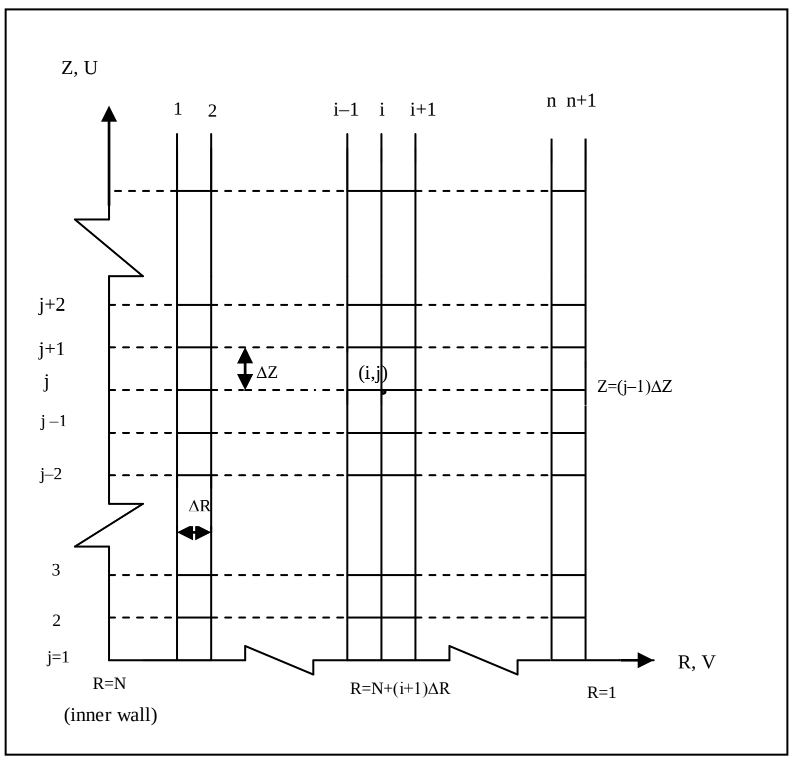

Fig.2: Mesh network of finite difference representation.

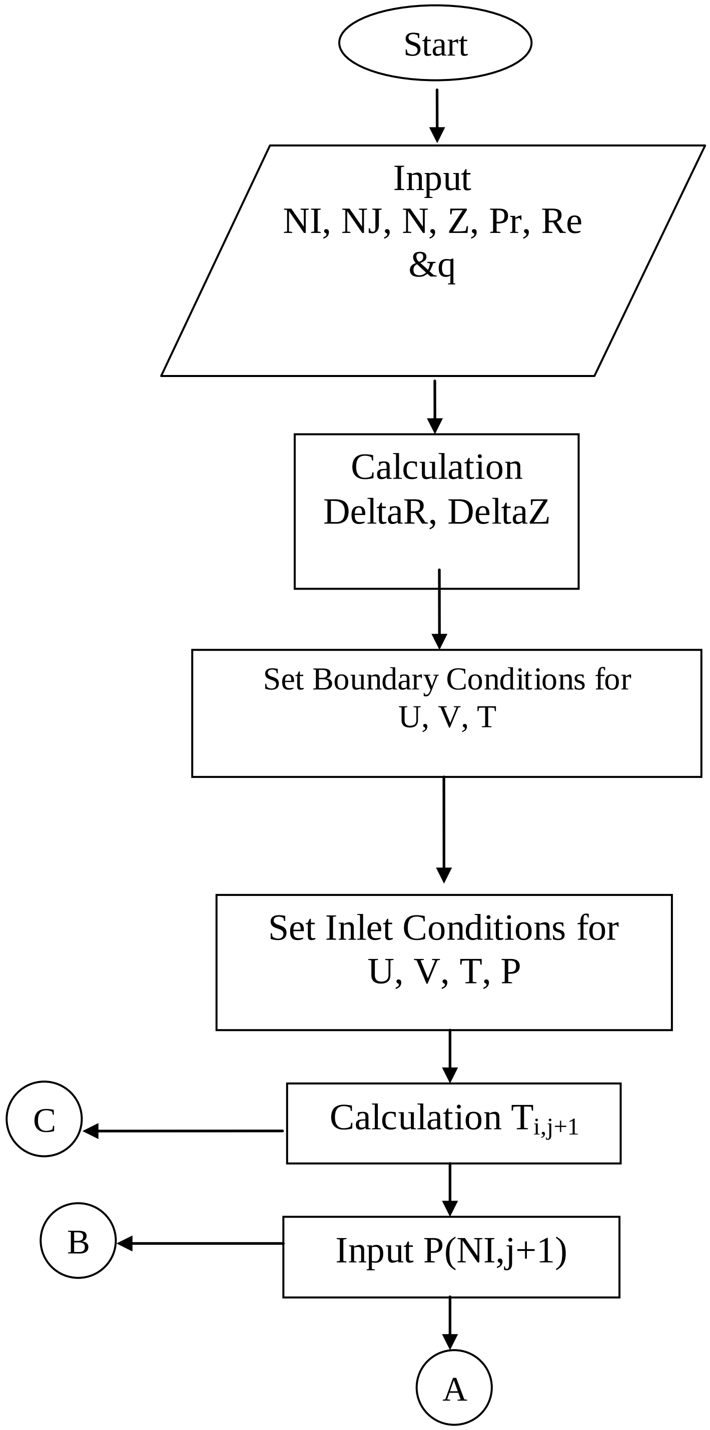
Start
Input
NI, NJ, N, Z, Pr, Re
&q
Calculation
DeltaR, DeltaZ
Set Boundary Conditions for
U, V, T
Set Inlet Conditions for
U, V, T, P
Calculation $T_{i,j+1}$
C
Input P(NI,j+1)
B
A

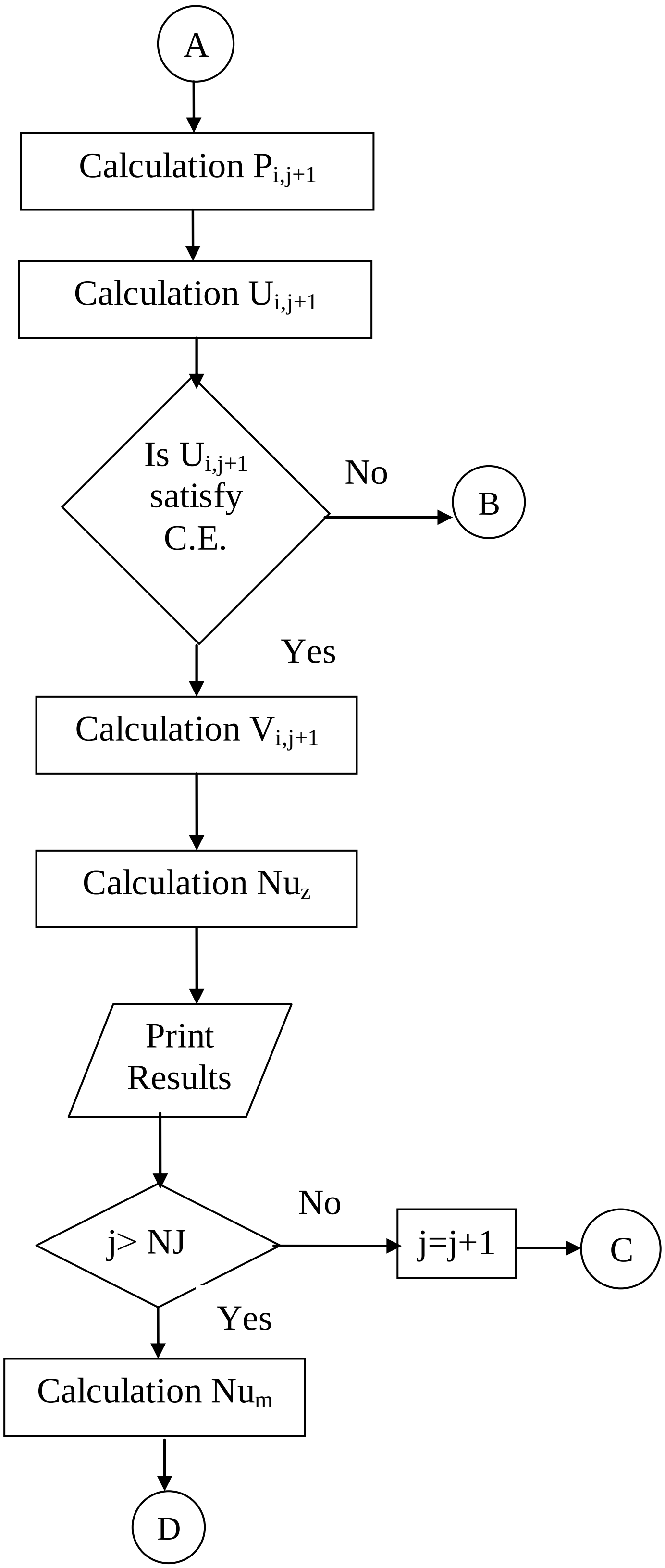
A
Calculation $P_{i,j+1}$
Calculation $U_{i,j+1}$
Is $U_{i,j+1}$ satisfy C.E.
No
B
Yes
Calculation $V_{i,j+1}$
Calculation Nu_z
Print Results
j> NJ
No
j=j+1
C
Yes
Calculation Nu_m
D

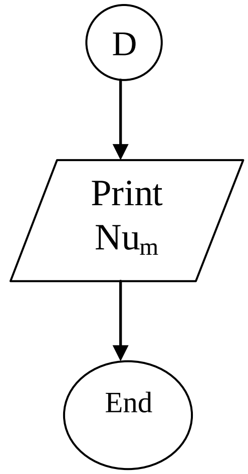

Fig .(3)Flow Chart of Computer Program

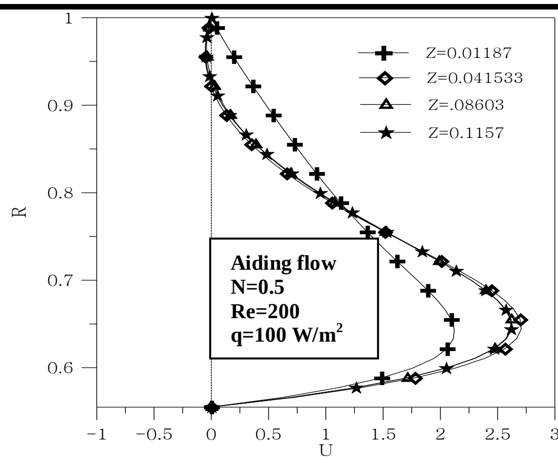

Fig.(4) Development of the axial velocity profiles at various positions along the annulus, for aiding flow, N=0.5, q=100 W/m^2, Re=200.

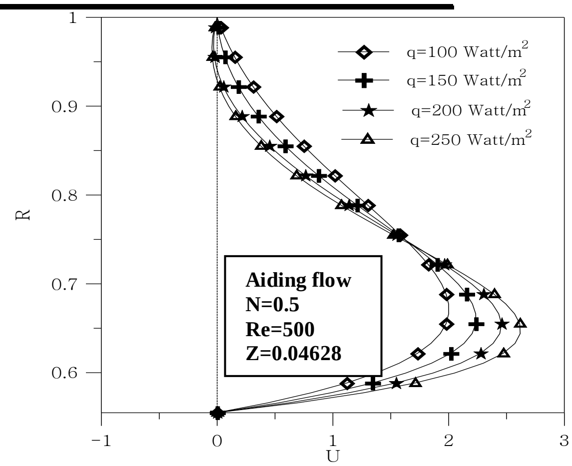

Fig.(6) Development of the axial velocity profiles at various positions along the annulus, for aiding flow, N=0.5, Z=0.04628, Re=500.

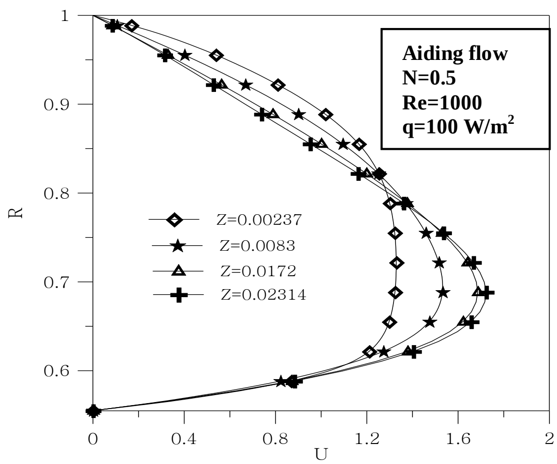

Fig. (5) Development of the axial velocity profiles at various positions along the annulus, for aiding flow, N=0.5, q=100 W/m^2, Re=1000.

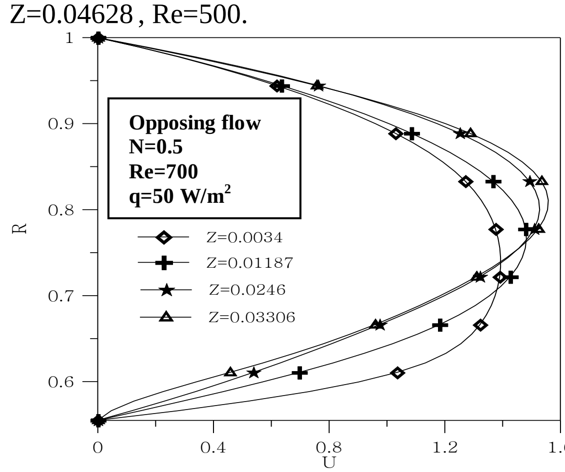

Fig.(7) Development of the axial velocity profiles at various positions along the annulus, for opposing flow, N=0.5, q=50 W/m^2, Re=700.

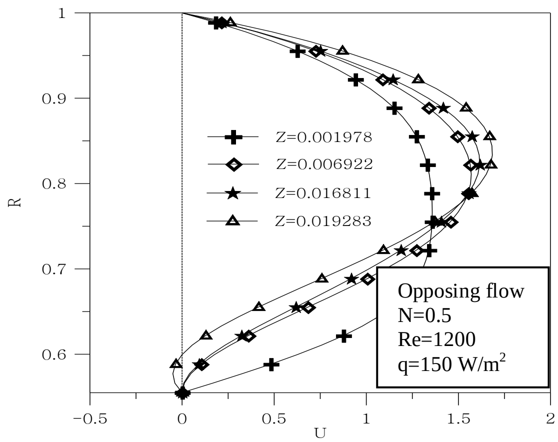

Fig.(8) Development of the axial velocity profiles at various positions along the annulus for opposing flow, N=0.5, q=150 W/m^2, Re=1200.

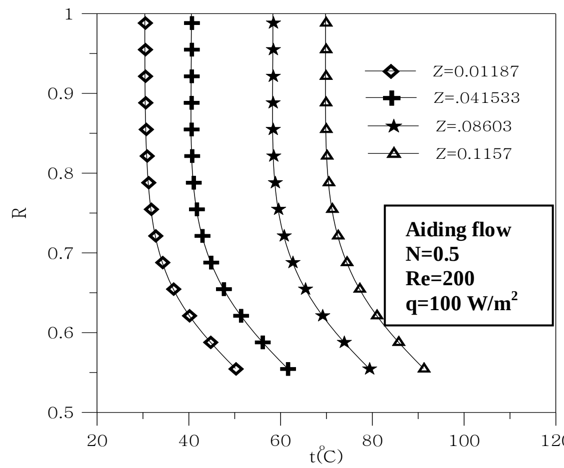

Fig.(10) Development of the temperature profiles at various positions along the annulus, for aiding flow, N=0.5, q=100 W/m^2, Re=200.

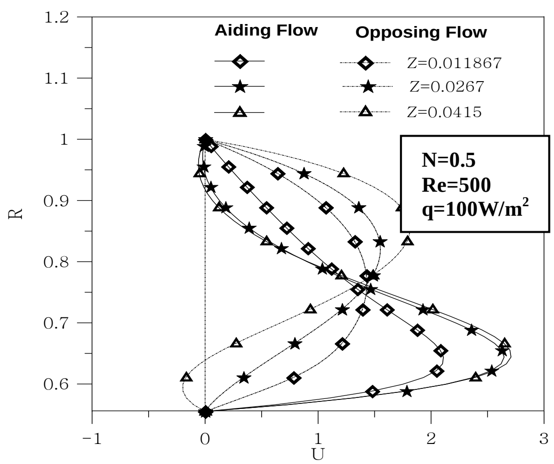

Fig.(9) Development of the axial velocity profiles at various positions along the annulus for aiding and opposing flows , N=0.5, q=100 W/m^2, Re=500.

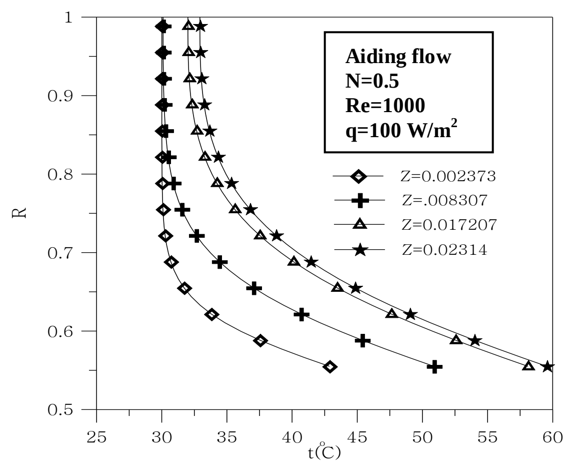

Fig.(11) Development of the temperature profiles at various positions along the annulus, for aiding flow, N=0.5, q=100 W/m^2, Re=1000.

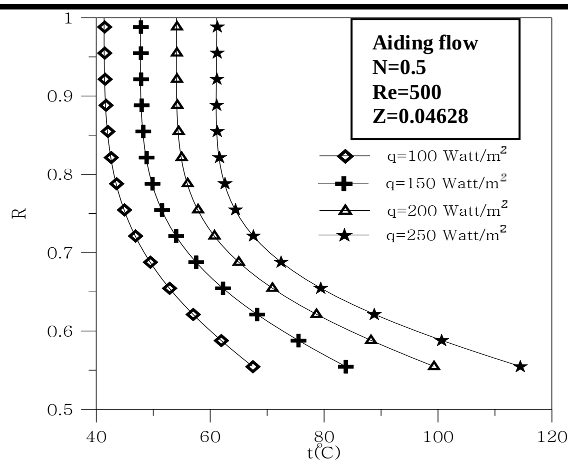

Fig.(12) Development of the axial temperature profiles at Z=0.04628, for aiding flow, N=0.5, Re=500.

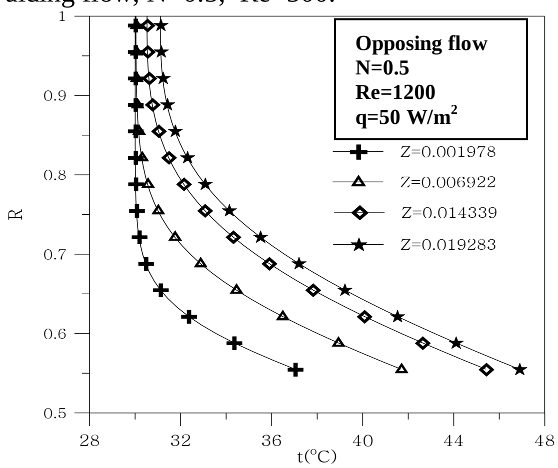

Fig.(13) Development of the temperature profiles at various positions along the annulus, for opposing flow, N=0.5, q=50 W/m^2, Re=1200.

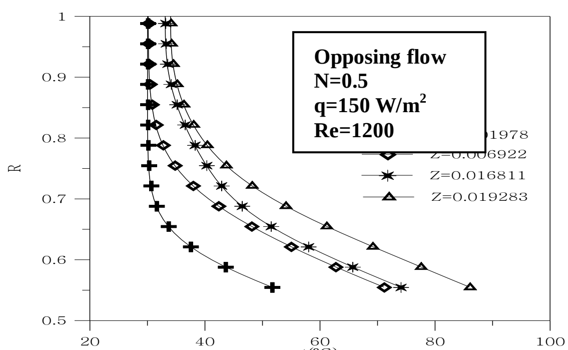

Fig.(14) Development of the temperature profiles at various positions along the annulus, for opposing flow, N=0.5, q=150 W/m^2, Re=1200.

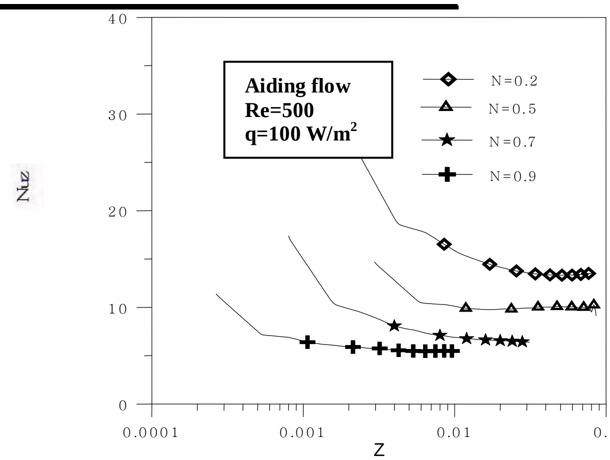

Fig.(15) Local Nusselt number versus dimensionless axial distance, for aiding flow, q=100 W/m^2, Re=500.

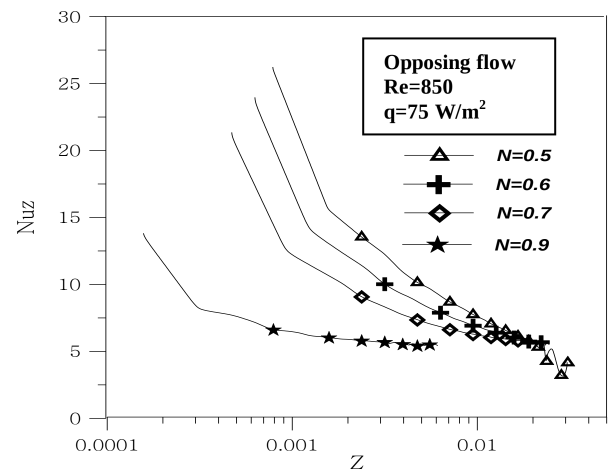

Fig.(16) Local Nusselt number versus dimensionless axial distance, for opposing flow, q=75 W/m^2, Re=850.

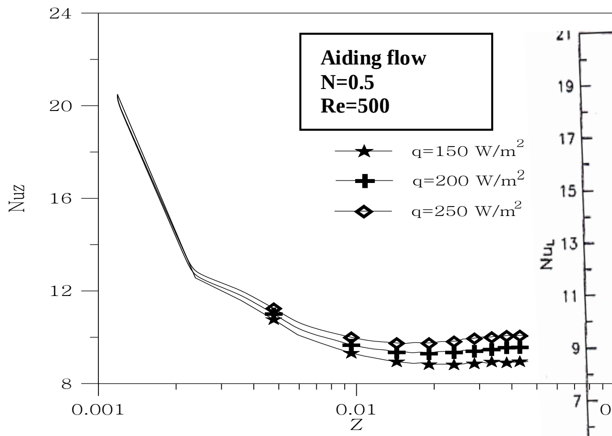

Fig.(17) Local Nuslt number versus dimensionless axial distance, for aiding flow, N=0.5 , Re=500.

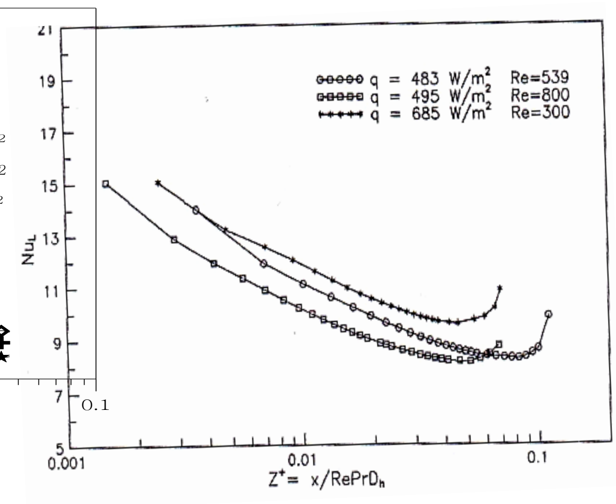

Fig.(20) Local Nusselt number at various positions along annulus for different heat fluxes and Reynolds numbers [Falah 1993].

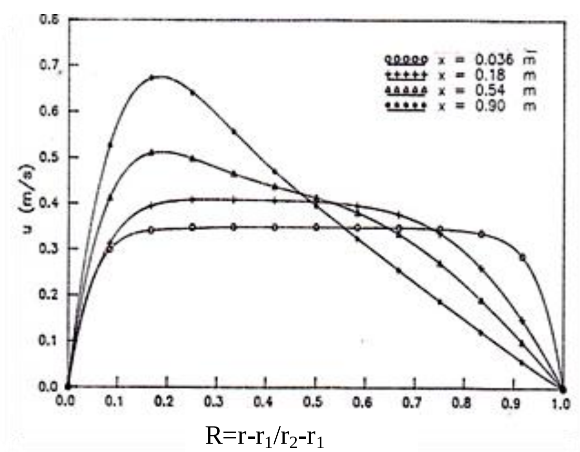

Fig.(18) Development of axial velocity profile for q=90 W/m^2 and Re=1200 [Falah 1993].

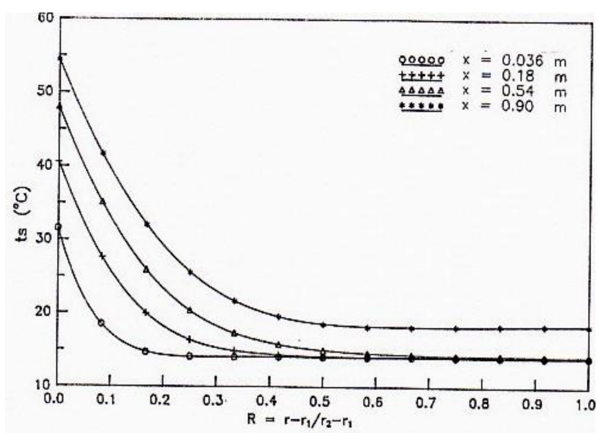

Fig.(19) Development of temperature profile at various positions along annuls for q=90 W/m^2 and Re=300 [Falah 1993].